Polydatin prevents bleomycin-induced pulmonary fibrosis by inhibiting the TGF-β/Smad/ERK signaling pathway

YAN-LU LIU[1*], BAO-YI CHEN[1*], JUAN NIE[1], GUANG-HUI ZHAO[1], JIAN-YI ZHUO[1], JIE YUAN[1,2], YU-CUI LI[1,2], LING-LI WANG[1,2**] and ZHI-WEI CHEN[1,2**]

[1]Mathematical Engineering Academy of Chinese Medicine, Guangzhou University of Chinese Medicine; [2]Guangdong Provincial Key Laboratory of New Drug Development and Research of Chinese Medicine, Guangzhou University of Chinese Medicine, Guangzhou, Guangdong 510006, P.R. China

Received August 25, 2019; Accepted May 13, 2020

DOI: 10.3892/etm.2020.9190

Abstract. Idiopathic pulmonary fibrosis (IPF) is a chronic, progressive, irreversible interstitial lung disease, with no effective cure. Polydatin is a resveratrol glucoside with strong antioxidant, anti-inflammatory and anti-apoptotic properties, which is used for treating health-related disorders such as cardiac disabilities, various types of carcinoma, hepatitis and hepatic fibrosis. The present study aimed to investigate the protective effect of polydatin against bleomycin-induced IPF and the possible underlying mechanism. A549 cells were treated with transforming growth factor-β1 (TGF-β1) and polydatin to observe phenotypic transformation and the related gene expression was detected. Sprague-Dawley rats were divided into seven groups and intratracheally infused with bleomycin to establish a pulmonary fibrosis model (the sham control group received saline). The rats were given pirfenidone (50 mg/kg), resveratrol (40 mg/kg) and polydatin (10, 40 and 160 mg/kg) for 28 days. The results demonstrated that polydatin had low toxicity to A549 cells and inhibited TGF-β1-induced phenotypic transformation as determined by MTS assay or observed using a light microscope. It also decreased the gene expression levels of α-smooth muscle actin and collagen I and increased the gene expression levels of epithelial cell cadherin *in vitro* and *in vivo* by reverse transcription-quantitative PCR. Furthermore, polydatin ameliorated the pathological damage and fiber production in lung tissues found by hematoxylin and eosin staining and Masson trichrome staining. Polydatin administration markedly reduced the levels of hydroxyproline, tumor necrosis factor-α, interleukin (IL)-6, IL-13, myeloperoxidase and malondialdehyde and promoted total superoxide dismutase activity in lung tissues as determined using ELISA kits or biochemical reagent kits. It inhibited TGF-β1 expression and phosphorylation of Smad 2 and 3 and ERK-1 and -2 *in vivo* as determined by western blot assays. These results suggest that polydatin protects against IPF via its anti-inflammatory, antioxidant and antifibrotic activities, and the mechanism may be associated with its regulatory effect on the TGF-β pathway.

Correspondence to: Dr Zhi-Wei Chen, Guangdong Provincial Key Laboratory of New Drug Development and Research of Chinese Medicine, Guangzhou University of Chinese Medicine, 232 Waihuandong Road, Guangzhou, Guangdong 510006, P.R. China
E-mail: vitas_chan@126.com

[*,**]Contributed equally

Key words: idiopathic pulmonary fibrosis, polydatin, transforming growth factor-β1, epithelial-mesenchymal transition, anti-inflammatory, antioxidant

Introduction

Idiopathic pulmonary fibrosis (IPF) is a chronic, irreversible and lethal interstitial lung disease (1). People diagnosed with this disease survive for <3-5 years (2). Following inflammation and oxidative injury, abnormal myofibroblast activation is observed, accompanied by enhanced epithelial-mesenchymal transition (EMT) and a large amount of collagen is secreted for post-injury repair (3,4). This leads to excessive deposition of the extracellular matrix (ECM), collapse of alveolar structures, infiltration of inflammatory cells in the alveolar cavity and eventual development of interstitial fibrosis (5). Finally, the lung structure is destroyed, lung function is lost and breathing becomes difficult (6). It can lead to irreversible respiratory failure and eventually mortality (7). At present, no treatment exists for IPF. In addition, the anti-inflammatory and immunosuppressive effects of traditional drugs are not clinically optimistic and serious side effects always occur (8). Therefore, a drug with significant efficacy and few side effects needs to be developed urgently.

Resveratrol (3,4',5-trihydroxystilbene; Fig. 1A), a natural phytoalexin, is abundant in a variety of plants such as grapes, peanuts and berries and also in a number of commercial products such as grape juice and red wine (9). It is a stilbene compound with a strong antioxidant property owing to its polyphenol structure (10). Previous studies provide abundant basic data for the use of resveratrol against lung disease (11) and fibrosis disease (12). Further, resveratrol exerts a protective effect against pulmonary fibrosis by inhibiting the proliferation and differentiation of lung fibroblasts and reducing the deposition of collagen (13). However, it has poor water solubility

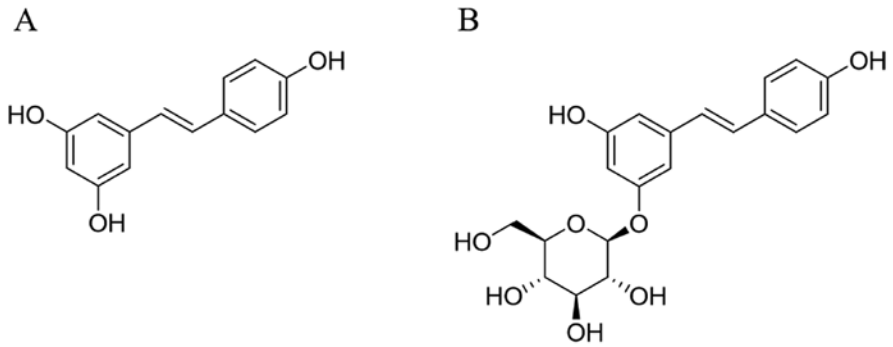

Figure 1. Chemical structures of (A) resveratrol and (B) polydatin.

due to its molecular structure, limiting its bioavailability and pharmaceutical applications (14).

Polydatin (3,4',5-trihydroxystilbene-3-β-mono-D-gluco side; Fig. 1B) is a resveratrol glucoside (15). Polydatin is usually isolated from the roots of a Chinese medicinal herb *Polygonum cuspidatum* Sieb. et Zucc. (Polygonaceae) (16). It is also abundant in several common dietary products such as red wine, peanuts, grapes and cocoa products, making it a promising dietary supplement combined with other clinical antifibrotic drugs (17). Polydatin is more abundant than resveratrol in nature and usually serves as a direct precursor of resveratrol (18). Unlike resveratrol, polydatin is more soluble in water owing to the conformational changes in its structure in which the hydroxyl group is substituted by a glucoside group on position C-3 (Fig. 1B). Polydatin has much better bioavailability than resveratrol, benefiting from the way polydatin enters cells via glucose carriers (19). Hence, polydatin should have a wider range of applications and better biological properties than resveratrol. Studies have shown that it displays strong antioxidant, anti-inflammatory and anti-apoptotic properties. Thanks to these properties, polydatin is frequently used for treating health-related disorders such as cardiac disabilities (20), various carcinomas (21,22), hepatitis (23) and hepatic fibrosis (24). It can also significantly reduce lipopolysaccharide-induced lung injury (25), protect against PM2.5-induced respiratory system diseases (26) and alleviate reactive oxygen species (ROS)- and bleomycin (BLM)-induced EMT and pulmonary fibrosis (27,28).

Despite the amount of data on the role of resveratrol against pulmonary fibrosis, the effect of resveratrol glucoside polydatin on IPF has not been explored in any depth. Therefore, the present study aimed to compare the efficacy of resveratrol and its glucoside polydatin and further investigate the possible underlying mechanism of polydatin against BLM-induced IPF.

Materials and methods

Drugs and chemicals. Polydatin (purity >99%) and resveratrol (purity >99%) were purchased from Guangzhou Honsea Sunshine Biotech Co., Ltd. Bleomycin (BLM) hydrochloride was obtained from Zhejiang Hisun Pharmaceutical Co., Ltd. Pirfenidone was acquired from Dalian Meilun Biotechnology Co., Ltd. Recombinant human transforming growth factor-β1 was obtained from PeproTech Inc.; it was diluted and stored following the manufacturer's protocol. Sodium carboxymethylcellulose (CMC-Na) was supplied by Sigma-Aldrich (Merck KGaA). The assay kits for measuring hydroxyproline (HYP) and malondialdehyde (MDA) contents and total superoxide dismutase (T-SOD) and myeloperoxidase (MPO) activities were supplied by Nanjing Jiancheng Bioengineering Institute. Enzyme-linked immunosorbent assay (ELISA) kits for tumor necrosis factor-α (TNF-α), interleukin (IL)-6 and IL-13 were purchased from Shanghai Enzyme-linked Biotechnology Co., Ltd. Reverse transcription primers for glyceraldehyde-3-phosphate dehydrogenase (GAPDH), collagen type I α 1 (Col1α1), epithelial cell cadherin (E-cadherin) and α-smooth muscle actin (α-SMA) were provided by Sangon Biotech Co., Ltd. Antibodies against β-actin, transforming growth factor-β1 (TGF-β1), phosphorylated *Drosophila* mothers against decapentaplegic protein homolog 2/3 (p-Smad2/3), Smad2/3, phospho-extracellular-regulated protein kinases 1/2 (p-ERK1/2) and ERK1/2 were supplied by Affinity Biosciences. Horseradish peroxidase (HRP) and goat anti-rabbit immunoglobulin G (H+L) were purchased from EarthOx, LLC. All other chemicals and reagents were at least of the analytic grade.

Cell culture. Human type II alveolar epithelial cell line A549 (American Type Culture Collection) was purchased from iCell Bioscience Inc. It was cultured in Roswell Park Memorial Institute-1640 (RPMI-1640) medium (Gibco; Thermo Fisher Scientific, Inc.) containing 10% (v/v) fetal bovine serum (Gibco; Thermo Fisher Scientific, Inc.) and 1% (v/v) penicillin/streptomycin solution (Gibco; Thermo Fisher Scientific, Inc.) at 37˚C, in a humidified atmosphere of 5% CO_2.

Cellular toxicity detection. The A549 cells were seeded in a 96-well plate at a density of $4x10^4$ cells/ml at 100 μl per well. Then, they were treated with polydatin (0-120 μM) for 24, 48, 72 and 96 h. Next, 20 μl of thiazolyl blue tetrazolium bromide (MTT; 5 mg/ml) was added to each well. Following incubation for 4 h, MTT was removed and 150 μl of dimethyl sulfoxide (DMSO) was added to each well. The 96-well plate was shaken on a microplate reader (Thermo Fisher Scientific, Inc.) for 10 min to dissolve the crystals completely. The absorbance was recorded at 490 nm using a microplate reader. The experiment was repeated three times.

Morphological observation and RNA extraction. The A549 cells were seeded in a 6-well plate at a density of $4x10^4$ cells/ml at 2 ml per well. Then, they were treated with 0, 10, 30 and

Table I. Primer sequences used for quantitative PCR.

Gene name		Primer (5'-3')
Human-GAPDH	Forward	GGCACCGTCAAGGCTGAGAAC
	Reverse	GGTGGCAGTGATGGCATGGAC
Human-Col 1a1	Forward	CCTGCCGTGACCTCAAGATGTG
	Reverse	CATGCTCTCGCCGAACCAGAC
Human-E-cadherin	Forward	TACAATGCCGCCATCGCTTACAC
	Reverse	TGACGGTGGCTGTGGAGGTG
Human-α-SMA	Forward	TCGTGCTGGACTCTGGAGATGG
	Reverse	CCGATGAAGGATGGCTGGAACAG
Rat-GAPDH	Forward	GTCCATGCCATCACTGCCACTC
	Reverse	CGCCTGCTTCACCACCTTCTTG
Rat-Col 1a1	Forward	GACAGGCGAACAAGGTGACAGAG
	Reverse	TGAGGTGGCTGAGGCAGGAAG
Rat-E-cadherin	Forward	GCTGCCATCGCCTACACCATC
	Reverse	ACCGACCTCATTCTCAAGCACTTG
Rat-α-SMA	Forward	AGAACACGGCATCATCACCAACTG
	Reverse	TGAGTCACGCCATCTCCAGAGTC

α-SMA, α-smooth muscle actin; GAPDH, glyceraldehyde-3-phosphate dehydrogenase; Col1α1, collagen type I α 1.

90 μM polydatin combined with TGF-β1 (10 ng/ml) for 96 h. The cells were acquired after 96 h. TRIzol® reagent (Invitrogen; Thermo Fisher Scientific, Inc.) was added to extract the total RNA according to the manufacturer's protocol.

Animal experiments. A total of 42, six-week-old specific-pathogen-free male Sprague-Dawley rats (180-220 g) were provided by Guangdong Medical Laboratory Animal Center (certificate no. SYXK2018-0085). The rats were maintained in the animal experimental center of Guangzhou University of Chinese medicine with five animals housed per cage. They were placed at a constant temperature of 24˚C, relative humidity of 65±15% and a 12-h light/dark cycle. They were given standard food and free drinking water. Animal health and behavior were monitored every day. All experimental protocols were in accordance with the regulations of the Animal Protection and Use Committee of Guangzhou University of Chinese Medicine.

BLM-induced IPF in rats. The rats were given adaptive feeding for 1 week before starting the experiment. They were randomly divided into seven groups: Sham control, model, pirfenidone, resveratrol and polydatin low-, medium- and high-dose groups, with six rats in each group. BLM-induced IPF was performed as described in a previous study (29). The rats were anesthetized with 50 mg/kg pentobarbital sodium by intraperitoneal injection. Following anesthesia, the anterior neck region of the rats was shaved and disinfected. Blunt dissection was made to expose the trachea. Then, 5 mg/kg BLM hydrochloride was intratracheally instilled into the rats in the six BLM-induced groups. The sham control group received the same treatment with sterile saline. The rats were shaken vertically for 3 min for a uniform distribution. The subcutaneous tissue and skin were carefully sutured.

Drug intervention. Then, 3 days following surgery (to minimize suffering and distress of the rats), the sham control and model groups were given 0.5% CMC-Na orally, the pirfenidone group was given 50 mg/kg pirfenidone, the resveratrol group was given 40 mg/kg resveratrol and the polydatin low-, medium- and high-dose groups were given 10, 40 and 160 mg/kg polydatin, respectively, once a day for 28 days. Both polydatin and resveratrol were dissolved in 0.5% CMC-Na solution. As described in a previous study (30), on the 28th day following BLM administration, the degree of IPF in rats was obvious and the vital signs were affected. Therefore, this was chosen as the humane endpoint. Following the last administration, the animals were euthanized with 200 mg/kg pentobarbital sodium by intraperitoneal injection. When the rats were anesthetized, the blood of the rats was drained. After draining the blood and arresting the cardiac and respiratory functions, the lung tissues were rapidly stripped for further study.

Histopathological evaluation. The lung tissues were fixed with 4% paraformaldehyde for 24 h at room temperature. The lung tissues were dehydrated with an alcohol gradient (75% alcohol 4 h, 85% alcohol 2 h, 90% alcohol 2 h, 95% alcohol 1 h and anhydrous ethanol 1 h). Xylene is used to make the tissue transparent. They were then immersed in melted paraffin at 65˚C for 3 h, before embedding in a frame filled with molten paraffin and allowed to solidify at -20˚C. Paraffin-embedded tissue blocks were cut into 4-μm sections. These sections were stained with hematoxylin and eosin (H&E) reagent, hematoxylin (0.5%) for 5 min, followed by eosin (0.5%) for 5 min; or with Masson's trichrome reagent, sequentially with potassium dichromate (10%) overnight, iron-hematoxylin (1%) for 3 min, Ponceau acid (1%) for 10 min, phosphomolybdic acid (1%) stain for 3 min and aniline blue (1%) for 6 min; all at room

temperature and observed under a light microscope. The lung injury scores were calculated according to the degrees of interstitial inflammation, inflammatory cell infiltration, congestion and edema. The scores on these indicators ranged 1-4. The final lung injury score was the sum of these scores (31). The lung fibrosis changes were evaluated according to the modified Ashcroft method (grades 0-8) (32). At scores 1-3, the alveoli were partly enlarged and rarefied. Fibrotic masses appeared from score 4. The lung structure was severely damaged with the confluence of single fibrotic masses at score 5. Most of the lung structure was not preserved at score 6. At score 7, the alveoli were partially covered by fibrotic masses and at score 8, complete occlusion occurred (33).

Reverse transcription-quantitative (RT-q)PCR. Total RNA of the rat lung tissues was extracted using TRIzol® reagent. The total RNA of cells ($5x10^5$) and lung tissues was reverse transcribed to cDNA (reaction volume, 20 μl) using the HiScript II Q RT SuperMix (Vazyme Biotech Co., Ltd.). An Ultra-trace UV-Visible spectrophotometer (Invitrogen; Thermo Fisher Scientific, Inc.) was used to detect the concentration and purity of RNA. The sample variation was amplified and quantified (reaction volume, 20 μl) using an SYBR quantitative polymerase chain reaction Master Mix kit (Vazyme Biotech Co., Ltd.). cDNA was subjected to a temperature of 95˚C for 30 sec; 40 cycles at 95˚C for 10 sec and 60˚C for 30 sec; and then 95˚C for 15 sec, 60˚C for 60 sec and 95˚C for 15 sec. The sequences of the primer are shown in Table I. GAPDH was used as an internal reference. RNA extraction, cDNA synthesis and qPCR were performed according to the manufacturer's protocols. The relative gene expression of Col I, E-cadherin and α-SMA was calculated using the following formulas: $\Delta\Delta Cq=(Cq_{sample}-Cq_{GAPDH})-(Cq_{control}-Cq_{GAPDH})$; fold change=$2^{-\Delta\Delta Cq}$ (34).

Determination of HYP level. The content of HYP in lung tissues was measured according to the hydroxyproline assay kit protocol (35). The data are expressed as microgram of HYP per milligram wet lung weight (μg/mg tissue).

T-SOD, MDA and MPO assays. The activities of T-SOD and MPO and the contents of MDA in lung tissues were determined by the hydroxylamine, hydrogen peroxide and thiobarbituric acid methods. The levels were determined by the colorimetric method following the manufacturer's protocols (Nanjing Jiancheng Bioengineering Institute).

TNF-α, IL-6 and IL-13 assays. Saline was added to the lung tissues (100 mg) at a ratio of 1:9. The tissues were then homogenized and centrifuged to remove the supernatant. TNF-α (cat. no. ml002859), IL-6 (cat. no. ml102828) and IL-13 (cat. no. ml003012) ELISA kits (Shanghai Enzyme-linked Biotechnology Co., Ltd.) were used to detect the expression of these proteins following the manufacturer's protocols.

Western blot analysis. To collect the total proteins, the lung tissues were homogenized using preconfigured radioimmunoprecipitation assay (RIPA) cracking liquid [containing RIPA lysis buffer, phenylmethanesulfonyl fluoride (PMSF), cocktail and phosphatase inhibitors A and B at ratios of 100:1:2:1:1]. The supernatant was collected following centrifugation at 14,000 x g for 10 min at 4˚C. The concentrations of proteins were measured using a bicinchoninic acid assay kit. Proteins were loaded at 50 μg per lane. The proteins were dispersed using 8% sodium dodecyl sulfate-polyacrylamide gel electrophoresis and then transferred onto polyvinylidene fluoride membranes. The membranes were blocked for 1 h at room temperature in Tris buffer solution-0.1% Tween 20 (TBST) containing 5% skimmed milk powder. Subsequently, they were incubated with specific primary antibodies at 1:1,000 dilution [p-ERK1/2 (cat. no. AF1015), ERK1/2 (cat. no. AF0155) and β-actin (cat. no. AF7018)] and 1:2,000 dilution [p-Smad2/3 (cat. no. AF3367), Smad2/3 (cat. no. AF6367) and TGF-β1 (cat. no. AF1027)] overnight at 4˚C. The membranes were incubated for 1 h at room temperature in TBST containing HRP and goat anti-rabbit immunoglobulin G secondary antibody (cat. no. E03012001; EarthOx Life Sciences). The protein bands were detected using an enhanced chemiluminescence advanced kit (GE Healthcare). Quantity One (v4.6.2; Bio-Rad Laboratories, Inc.) was used for densitometry.

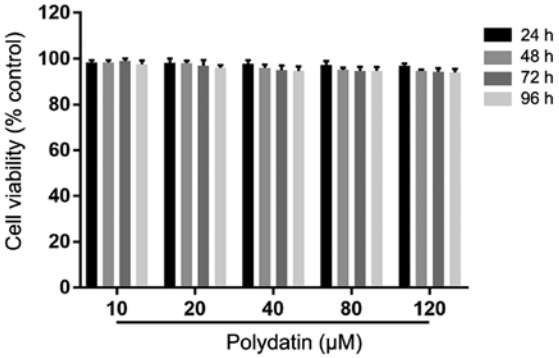

Figure 2. Effects of polydatin (0, 10, 20, 40, 8 and 120 μM) for 24, 48, 72 and 96 h on A549 cells. Values are represented as mean ± standard deviation (n=5).

Statistical analysis. SPSS software (version 23.0, IBM Corp.) was used for data analysis. One-way analysis of variance and Fisher's least significant difference test were used to analyze the significance of different groups. Values represented as mean ± standard deviation $P<0.05$ was considered to indicate a statistically significant difference. ChemDraw Professional v16.0 was used to draw chemical structures. GraphPad Prism software (v7; GraphPad Software, Inc.) was used to draw the graphs.

Results

Cellular toxicity of polydatin in A549 cells. The results demonstrated that the viability of A549 cells after administering polydatin (10-120 μM) for 24, 48, 72 and 96 h was more than 90%. This suggested that polydatin had low toxicity to A549 cells at 10-120 μM (Fig. 2).

Polydatin protects against TGF-β1-induced phenotypic transformation of A549 cells. Based on the results of the cell toxicity experiment, different concentrations (0, 10, 30 and 90 μM) of polydatin combined with TGF-β1 (10 ng/ml) were subsequently selected to investigate the effect of their independent or combined use on the phenotypic transformation of A549 cells for 96 h. The results showed no significant

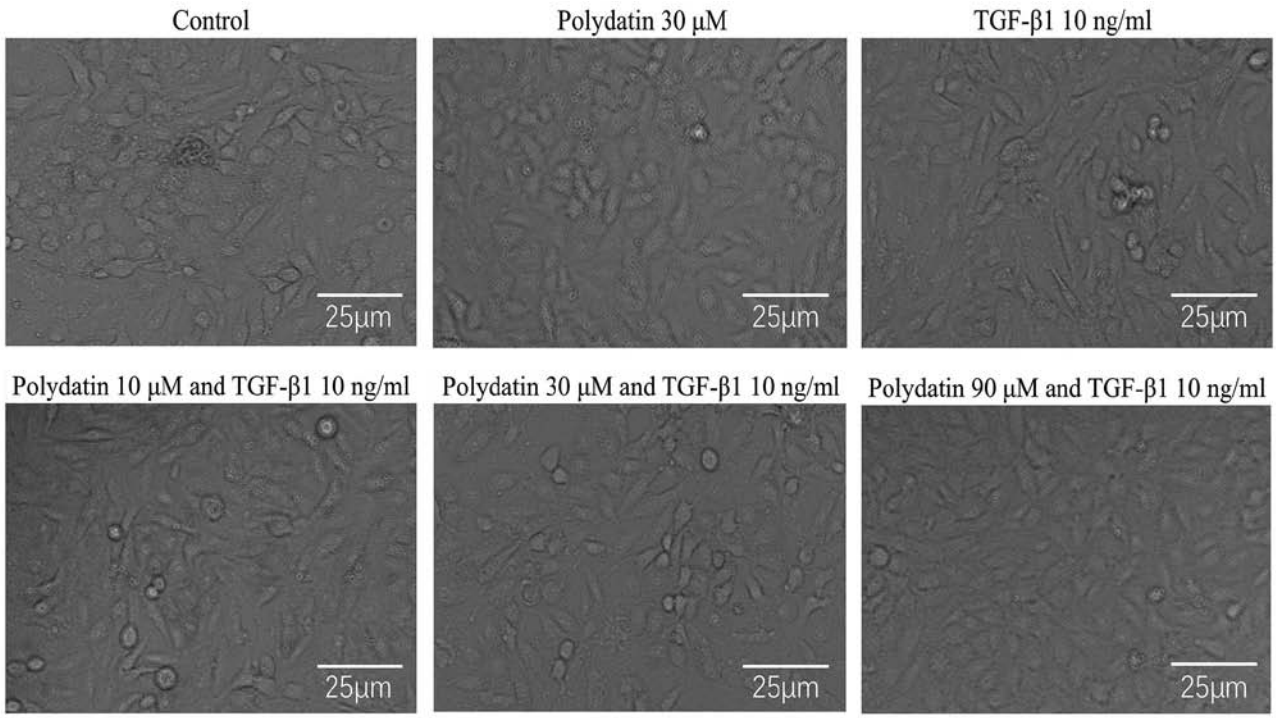

Figure 3. Effects of polydatin on the TGF-β1-induced phenotypic transformation of A549 cells (scale bars, 25 μm). TGF-β1, transforming growth factor-β1.

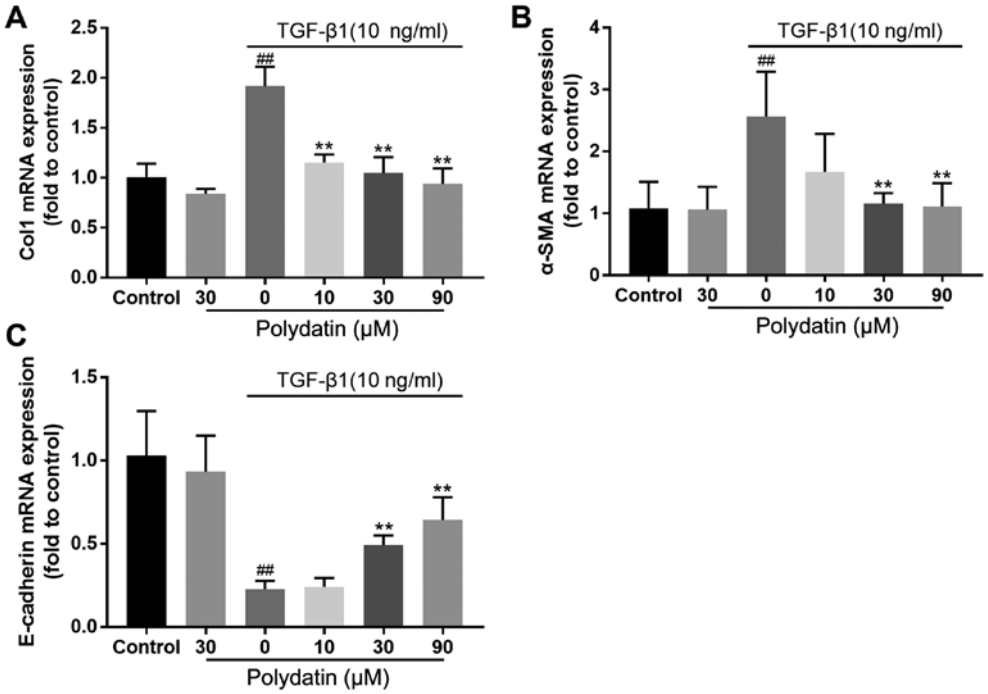

Figure 4. Effects of polydatin on EMT and fibrosis markers: (A) Col I, (B) α-SMA and (C) E-cadherin. Values are represented as mean ± standard deviation (n=6). ##P<0.01, the TGF-β1 alone administration group vs. the control group. **P<0.01, the polydatin and TGF-β1 combined administration group vs. the TGF-β1 alone group. EMT, epithelial-mesenchymal transition; Col I, collagen I; α-SMA, α-smooth muscle actin; TGF-β1, transforming growth factor-β1.

difference in cell morphology between the control and polydatin-administered groups. The epithelial cell phenotype in these two groups was anserine nephrite type. After 96 h, significant morphological differences were observed between the TGF-β1-treated and control groups; a number of the cells became spindle shaped in the TGF-β1 intervention group. Little difference in cell morphology was found between the polydatin (10 μM) combined with TGF-β1 group and the TGF-β1 intervention group during the experiment. However, the polydatin (30 and 90 μM) combined with TGF-β1 group showed significant morphological differences 96 h following the intervention; only a few cells were spindle shaped (Fig. 3).

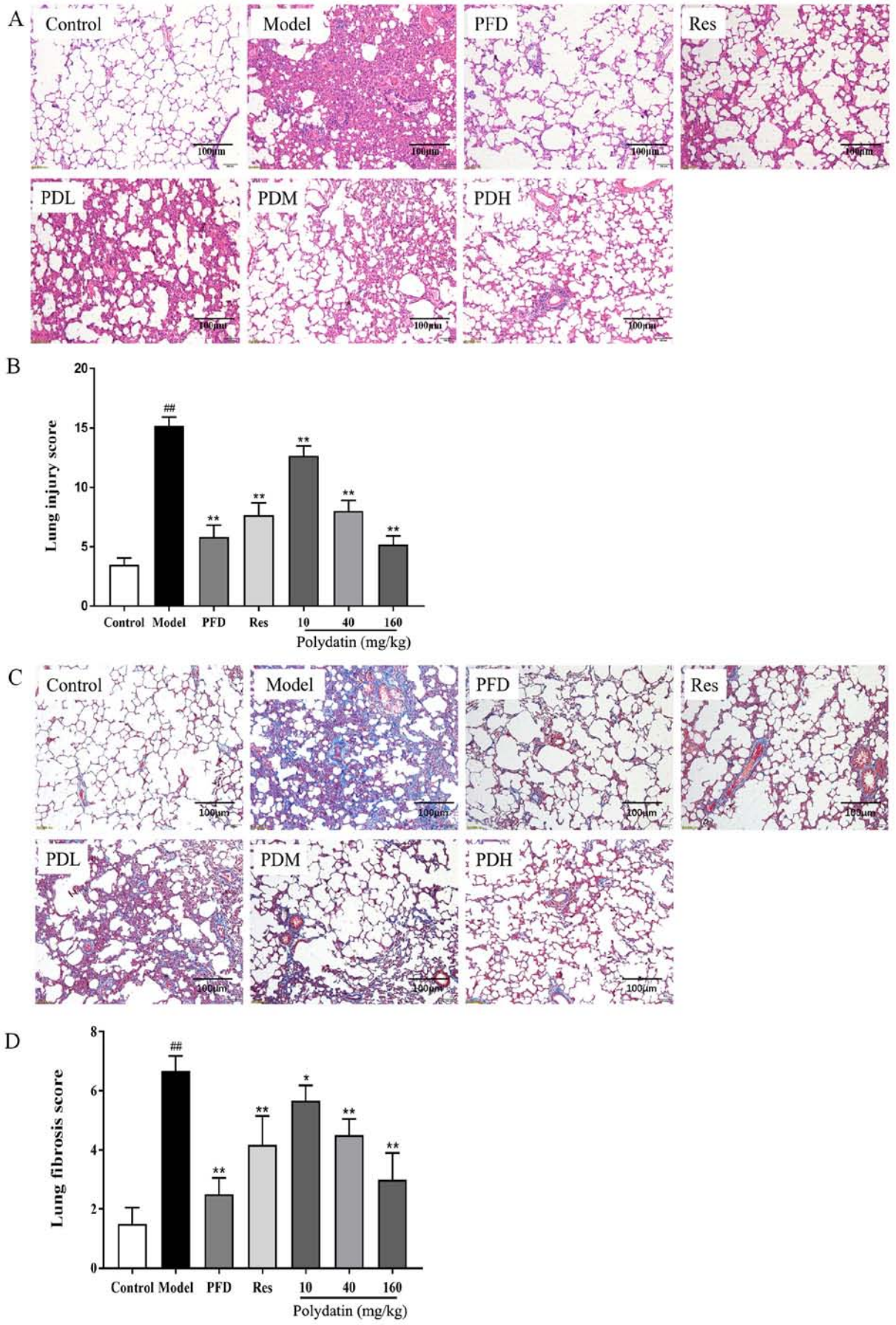

Figure 5. Effects of PFD, Res and polydatin on BLM-induced pathological damage and fibrogenesis. (A) H&E stain (scale bars, 100 μm). (B) Lung injury score. (C) Masson trichrome stain (scale bars, 100 μm). (D) Lung fibrosis score. Values are represented as mean ± standard deviation (n=6). $^{\#\#}$P<0.01, the model group vs. the control group. **P<0.01, *P<0.05, vs. the model group. PFD, pirfenidone; Res, resveratrol; BLM, bleomycin; PDL, PDM and PDH, polydatin low-, medium- and high-dose groups respectively.

Effect of polydatin on EMT of A549 cells. The results of phenotypic observation showed that the morphological differences among the groups were most obvious at 96 h following administration. Therefore, at 96 h following culture, total RNA was extracted from the cells in the polydatin and TGF-β1 alone or combined administration groups. The epithelial or mesenchymal marker gene was detected to reflect the EMT of the cells. The RT-qPCR results demonstrated no significant difference in the changes in the expression levels of collagen I (Col I), E-cadherin and α-SMA between the control and polydatin (30 μM) treatment groups. However, the expression of E-cadherin was significantly downregulated in the TGF-β1 (10 ng/ml) intervention group (P<0.01) and the expression of α-SMA and Col I was significantly increased (P<0.01), showing statistically significant differences compared with the control group. TGF-β1 (10 ng/ml) intervention combined with polydatin (30 and 90 μM) administration demonstrated significant differences in the expression of Col I, E-cadherin and α-SMA compared with TGF-β1 (10 ng/ml) intervention alone (P<0.01). The administration of polydatin inhibited the reduction in E-cadherin and the increase in Col 1 and α-SMA induced by TGF-β1. This inhibition displayed a dose-dependent trend (Fig. 4).

Polydatin ameliorates BLM-induced lung pathological damages and fibrogenesis in rats. *In vitro* experiments confirmed that polydatin significantly inhibited the TGF-β1-induced EMT of alveolar epithelial cells, which plays a crucial role in the pathogenesis of fibrosis. Therefore, a model of bleomycin-induced pulmonary fibrosis *in vivo* was established to verify whether polydatin had a protective effect on bleomycin-induced pulmonary fibrosis in rats. H&E staining revealed the most intuitive response to histopathological changes. The fibers in the tissue were stained blue by Masson trichome stain, directly reflecting the degree of organ fibrosis.

H&E staining showed that the model group had severe pulmonary structure collapse, alveolar structure consolidation, marked edema and congestion and inflammatory cell infiltration compared with the sham control group. Fortunately, pirfenidone (PFD), resveratrol (Res) and polydatin interventions reduced the pathological injury of lung tissue. They suppressed the alveolar wall damage and reduced inflammatory cell infiltration, congestion and edema (P<0.01). The effect of polydatin was dose-dependent. At the same dose, polydatin and resveratrol produced similar effects. However, higher doses of polydatin provided a stronger protective effect. All of these results are shown in Fig. 5A and B. Masson trichrome staining results showed that the lungs of rats treated with BLM had alveolar septal thickening and collapse, massive collagen deposition and fibrous hyperplasia compared with the sham control group (P<0.05). However, collagen deposition in the lungs was significantly reduced by pirfenidone (PFD), resveratrol (Res) and polydatin (P<0.01). Polydatin exerted the effect in a dose-dependent manner (P<0.05). The results are displayed in Fig. 5C and D.

Level of HYP. The results demonstrated that the content of HYP, a collagen deposition marker, significantly increased in the model group compared with the sham control group (P<0.01). However, pirfenidone (PFD) and resveratrol (Res) downregulated the expression of HYP (P<0.01). Polydatin also significantly blocked this induction in a dose-dependent manner (P<0.01; Fig. 6).

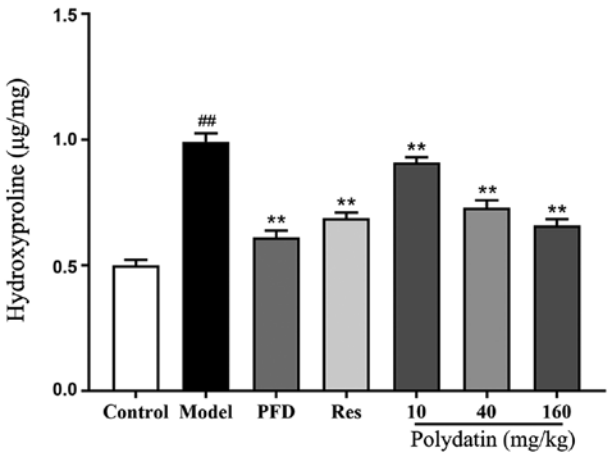

Figure 6. Effects of PFD, resveratrol Res and polydatin on the hydroxyproline level (μg/mg) in rats. Values are represented as mean ± standard deviation (n=6). ##P<0.01, the model group vs. the control group. **P<0.01, vs. the model group. PFD, pirfenidone; Res, resveratrol.

EMT and fibrosis markers are altered by polydatin during BLM-induced IPF. Fig. 7 shows that BLM significantly stimulated the gene expression of interstitial markers α-SMA and Col I and decreased the gene expression level of epithelial marker E-cadherin compared with rats having no BLM administration (P<0.01). However, pirfenidone (PFD), high- and medium-dose polydatin and resveratrol (Res) treatment significantly ameliorated the magnitude of all these changes at the mRNA level (P<0.01).

Polydatin protects against BLM-induced inflammatory injury in rats. BLM administration significantly elevated the levels of pro-inflammatory factors TNF-α, IL-6 and IL-13 in the lung homogenate compared with the sham control group. However, pirfenidone (PFD), resveratrol (Res) and polydatin (40 and 160 mg/kg) significantly decreased the elevated TNF-α, IL-6 and IL-13 levels (P<0.01) compared with the model group. Polydatin (10 mg/kg) also mitigated the lesions, but its effect was less compared with the other two doses of polydatin (P<0.01; Fig. 8).

Polydatin protects against BLM-induced oxidative damage in rats. Fig. 9 shows that BLM administration in rats caused increased oxidative stress as manifested by a significant decrease in T-SOD, and a significant increase in MDA levels and MPO activities in the lung tissues compared with the sham control group (P<0.01). Nevertheless, pirfenidone (PFD), resveratrol (Res) and polydatin (40 and 160 mg/kg) significantly overcame the BLM-mediated decrease in T-SOD and inhibited the BLM-mediated increase in MDA levels and MPO activities in the lung tissue (P<0.01) compared with the model group. Polydatin (10 mg/kg) also exerted the effect to a certain extent (P<0.05).

Polydatin downregulates the TGF-β/Smad/ERK signaling pathway during pulmonary fibrosis. Fig. 10 shows that

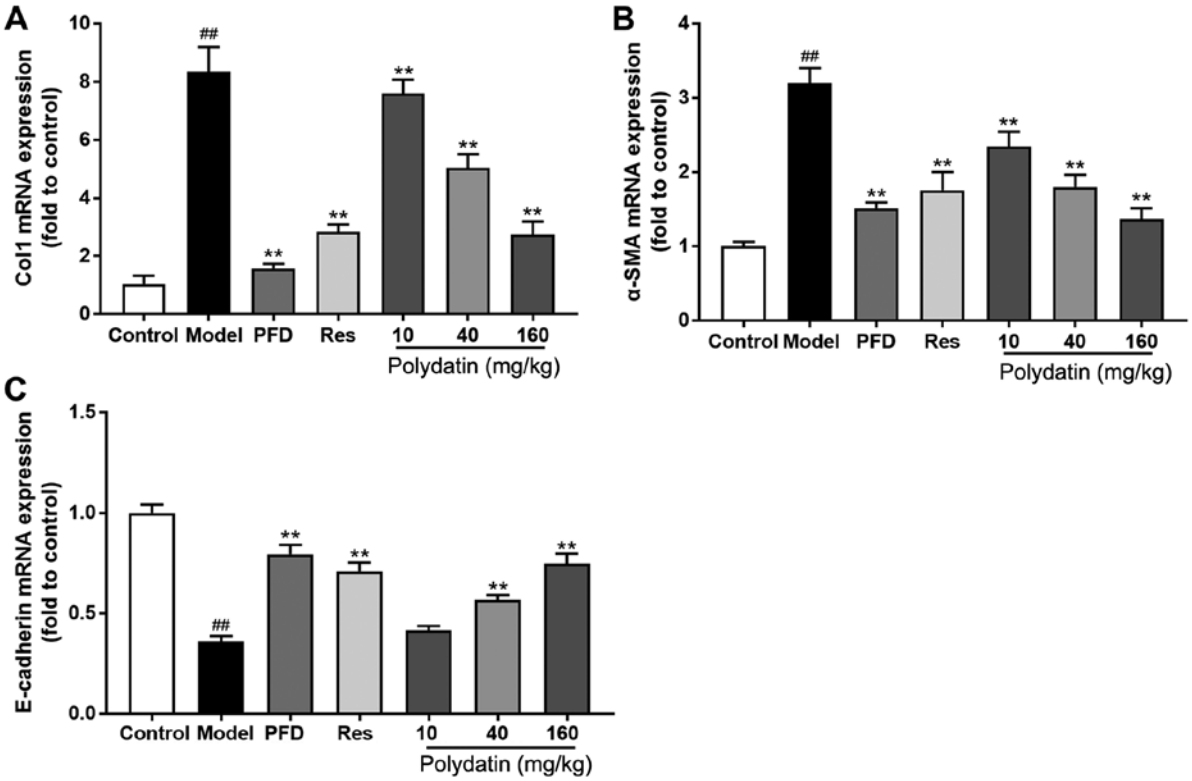

Figure 7. Effects of PFD, Res and polydatin on EMT and fibrosis markers: (A) Col I, (B) α-SMA and (C) E-cadherin. Values are represented as mean ± standard deviation (n=6). ##P<0.01, the model group vs. the control group. **P<0.01, vs. the model group. PFD, pirfenidone; Res, resveratrol; EMT, epithelial-mesenchymal transition; Col I, collagen I; α-SMA, α-smooth muscle actin.

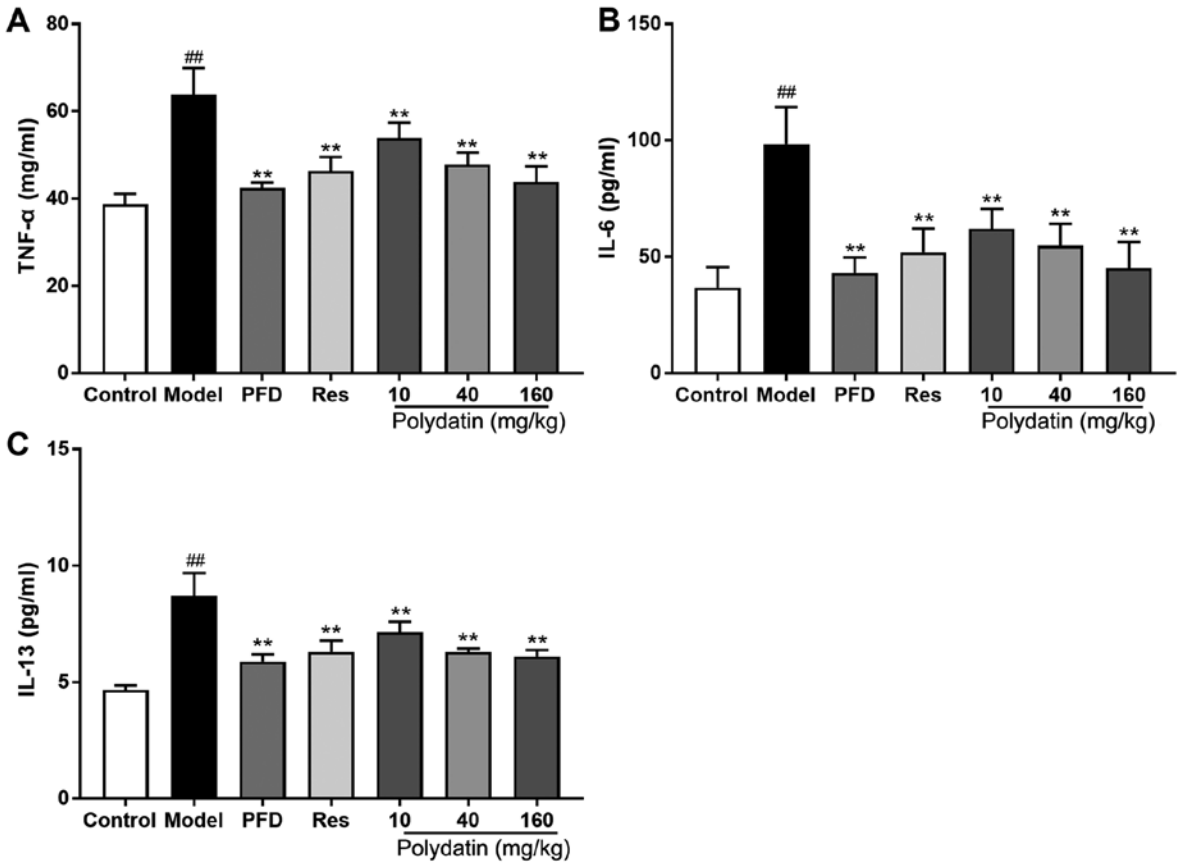

Figure 8. Effects of PFD, Res and polydatin on the levels of pro-inflammatory cytokines: TNF-α (A) IL-6 (B) and IL-13 (C) levels in rats. Values are represented as mean ± standard deviation (n=6). ##P<0.01, the model group vs. the control group. **P<0.01, vs. the model group. PFD, pirfenidone; Res, resveratrol; TNF-α, tumor necrosis factor-α; IL, interleukin.

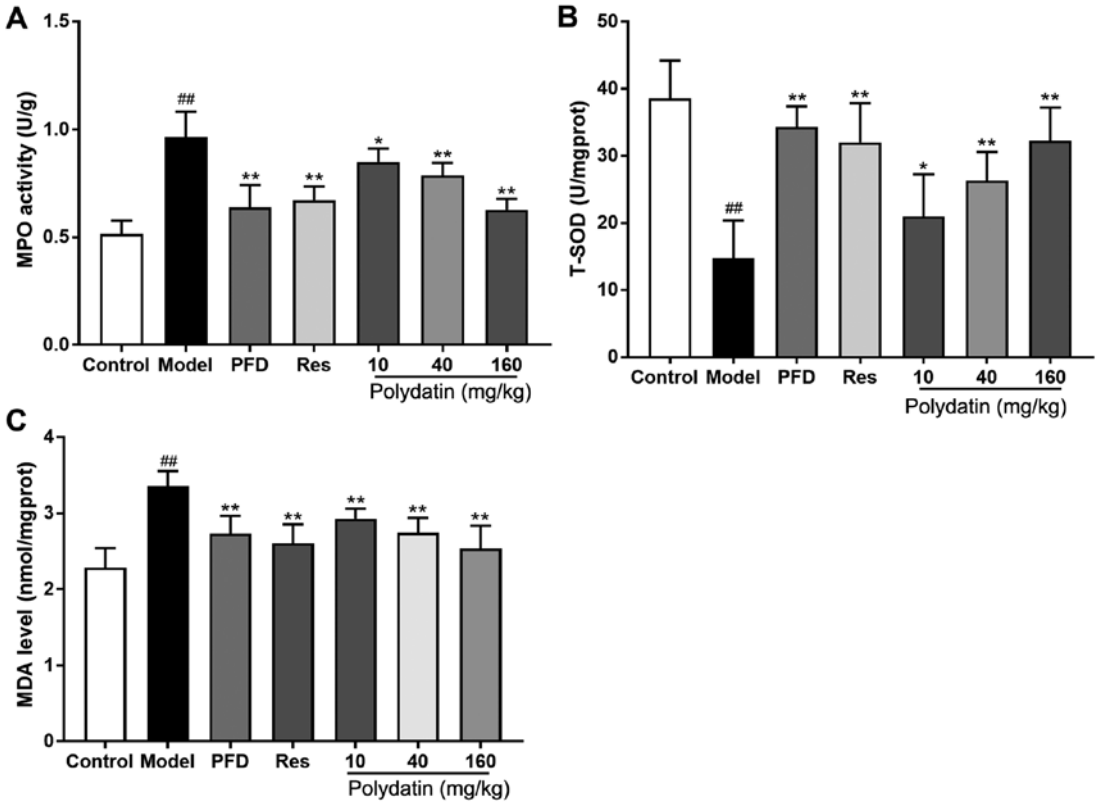

Figure 9. Effects of PFD, Res and polydatin on oxidative damage: (A) T-SOD, (B) MDA levels and (C) MPO activities. Values are represented as mean ± standard deviation (n=6). ##P<0.01, the model group vs. the control group. **P<0.01, *P<0.05, vs. the model group. PFD, pirfenidone; Res, resveratrol; T-, total; SOD, superoxide dismutase; MDA, malondialdehyde; MPO, myeloperoxidase.

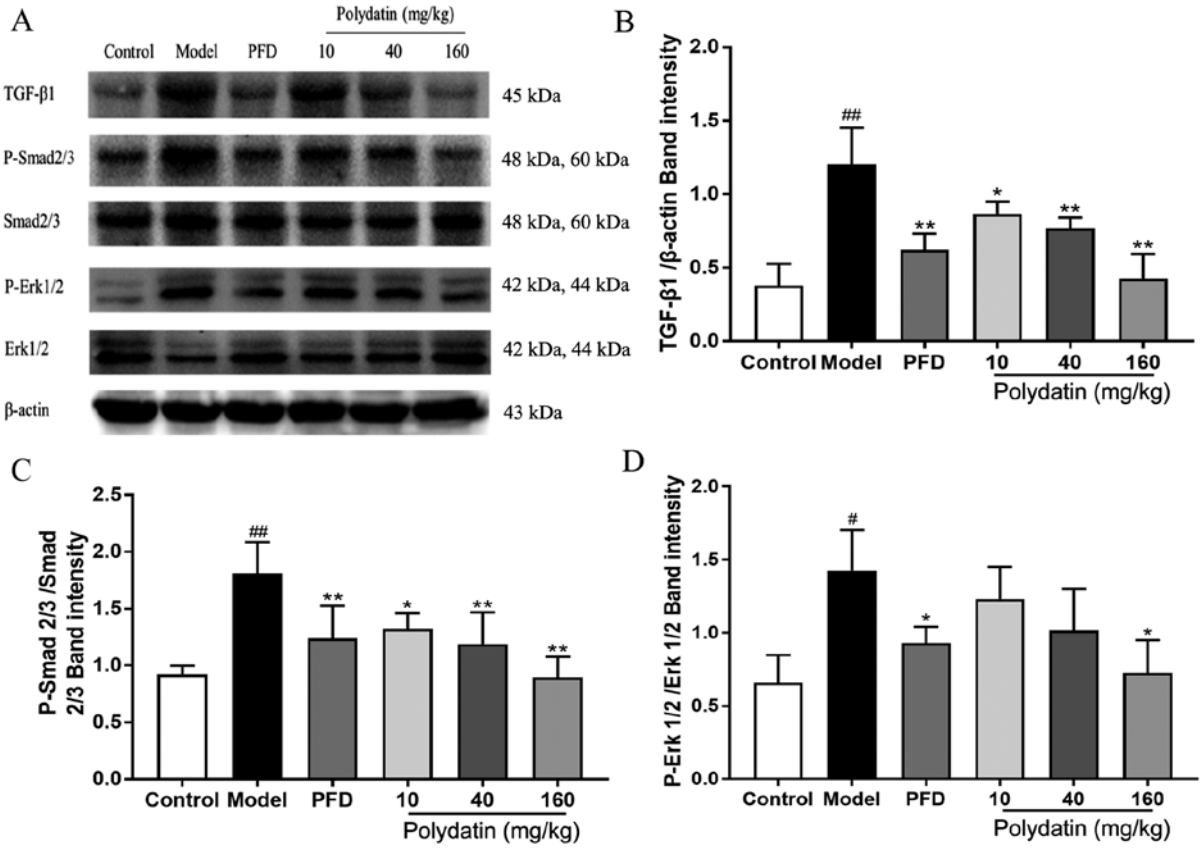

Figure 10. Effects of PFD and polydatin on the TGF-β/Smad/ERK signaling pathway. (A) Representative western blots and quantitative analysis of (B) TGF-β1/β-actin, (C) p-Smad2/3/Smad2/3 and (D) p-ERK1/2/ERK1/2 levels in rats. Values are represented as mean ± standard deviation (n=3). ##P<0.01 and #P<0.05, the model group vs. the control group. **P<0.01 and *P<0.05, vs. the model group. PFD, pirfenidone; TGF-β, transforming growth factor-β; p-, phosphorylated.

following BLM injection, the expression level of TGF-β1 and the phosphorylation of its downstream signals Smad2/3 and ERK1/2 were significantly increased in rats. Promisingly, polydatin was able to inhibit the elevation of the expression level of TGF-β1 and the phosphorylation of Smad2/3 and ERK1/2 in a dose-dependent manner ($P<0.05$).

Discussion

Idiopathic pulmonary fibrosis (IPF) is a chronic, progressive, irreversible clinical disease with survival of 3-5 years following diagnosis (36). At present, drugs for treating IPF are limited and no other means exist to cure the disease (37). IPF is characterized by the collapse and merging of alveolar structures, significant inflammatory cell infiltration, excessive collagen deposition and hyperplasia of fibers (38). The bleomycin (BLM)-induced pulmonary fibrosis model simulates the process and pathological characteristics of human pulmonary fibrosis on a larger scale (39). BLM dripping into the lung through the trachea directly causes severe lung injury (40). In the present study, massive alveolar septal thickening, alveolar wall collapse, inflammatory cell infiltration and fibrous hyperplasia occurred in the lungs of rats in the model group, confirming the devastating effect of BLM on the lungs. However, the treatment with polydatin effectively prevented lung tissue damage and the progression of pulmonary fibrosis. Its protective effect was reflected in less lung structure collapse, inflammatory cell infiltration, congestion and edema and prevention of collagen deposition and fiber formation in the treatment group. At the same time, polydatin significantly reduced the content of hydroxyproline (HYP) *in vivo* and collagen I (Col I) *in vitro* and *in vivo*, indirectly or directly reflecting its inhibitory effect on collagen synthesis. In addition, it also increased the expression level of epithelial marker E-cadherin and decreased the expression level of interstitial marker α-smooth muscle actin (α-SMA) *in vitro* and *in vivo*, reflecting its inhibitory effect on the epithelial-mesenchymal transition (EMT) process. The effect of polydatin was similar to that of pirfenidone and its aglycone resveratrol. In addition, higher doses of polydatin were more effective.

The formation of fibrosis is caused by excessive repair following injury induced by various harmful factors. Of these, oxidative damage and inflammatory damage are two extremely important sources. BLM stimulation can simulate the oxidative and inflammatory damage to human lung tissue (41,42). BLM injection directly and markedly damages alveolar epithelial cells (43). Inflammatory cells, such as neutrophils and macrophages, heavily infiltrate into the alveolar space (44), promoting the expression of TNF-α in alveolar epithelial cells and the expression of IL-1β, IL-13 and other pro-inflammatory factors (45). This causes a series of inflammatory responses and severe inflammatory injuries (46). At the same time, fibroblasts are activated in large numbers, secreting collagen proteins that can repair damage, and accumulate in the ECM, eventually leading to the formation of fibrotic lesions (47). In addition, the extent of inflammatory injury beyond repair can directly induce the apoptosis of alveolar epithelial cells (48). Therefore, inflammatory stress plays an important role in the development of fibrosis. However, neutrophil infiltration and activation release large amounts of myeloperoxidase (MPO) (49). Excessive MPO catalyzes the oxidation of protein tyrosine to produce oxidants such as 3-nitrotyrosine and 3-chlorotyrosine (50). When the oxidant production exceeds the local antioxidant defense reaction, it leads to oxidative stress and tissue oxidative damage (51). Meanwhile, *in vitro* studies confirmed that MPO oxidation products can trigger fibrocyte proliferation and promote fibrosis (52). In addition, BLM can directly attack DNA. BLM combines with iron to form an activated complex that promotes the production of oxidants such as reactive oxygen species (ROS) (53). ROS can indiscriminately attack DNA, proteins and lipids, causing severe oxidative damage (54). ROS can be oxidized by various fatty acids on the cell membrane to produce peroxide products such as MDA, resulting in decreased membrane stability and integrity, loss of function, cell damage and apoptosis (55).

Previous studies have demonstrated that polydatin possesses a strong anti-inflammatory activity. It resists LPS-induced pneumonia (19). The structure of polyphenol makes it possible for polydatin and resveratrol to have a strong antioxidant activity (56). The results of the present study demonstrated that BLM significantly increased the levels of TNF-α, IL-6 and IL-13 in rat lungs, suggesting that BLM induced a severe inflammatory response. The increase in the MPO level was another indication of neutrophil infiltration. In addition, the levels of MDA and SOD reflected the increase in oxidative stress and the decrease in the ability to scavenge oxygen free radicals. Following treatment with polydatin, the levels of pro-inflammatory factors TNF-α, IL-6 and IL-13, MPO and MDA were significantly decreased and the activity of SOD was increased. It was hypothesized that polydatin has certain anti-inflammatory and antioxidant activities and the mechanism may be related to inhibition of the secretion of inflammatory oxidative factors, enhancing the scavenging of oxygen free radicals and preventing the lipid peroxidation process. In contrast, the anti-inflammatory and antioxidant effects of polydatin were slightly lower compared with pirfenidone, a commonly used drug in clinical practice. However, its effect on reducing the levels of inflammatory factors was higher and its antioxidant effect was close to that of resveratrol at the same dose.

TGF-β1 has been found to regulate a wide array of cellular processes, including cell growth, differentiation, migration, apoptosis and ECM production (57,58). Particularly, it is considered a key mediator of fibrosis (59). The significant increase in TGF-β1 level in the lung tissue of rats with pulmonary fibrosis strongly demonstrated that TGF-β1 was closely related to pulmonary fibrosis (60). TGF-β could inhibit the growth of epithelial cells, re-program epithelial cells into mesenchymal cells and stimulate the production of ECM via regulating downstream regulators in pulmonary fibrosis (61,62). *In vitro* experiments demonstrated that 10 ng/ml TGF-β1 could significantly induce the transformation of type II alveolar epithelial cell A549 phenotype from cobblestone appearance into spindle-like appearance. This phenotypic transformation was accompanied by an increased expression level of Col I and mesenchymal marker α-SMA and decreased expression level of epithelial marker E-cadherin. It was proposed that TGF-β1 could induce the EMT process of alveolar epithelial cells and

promote collagen synthesis and deposition. Following the intervention of polydatin, alveolar epithelial cells retained their epithelioid phenotype and the decrease in the expression level of E-cadherin gene, an epithelial marker and the increase in the expression level of Col I and interstitial marker α-SMA were inhibited. This suggested that the protective effect of polydatin against pulmonary fibrosis might be related to the regulation via the TGF-β1 signaling pathway.

ROS produced by oxidative stress and pro-inflammatory factors, such as TNF-α, promotes the synthesis of TGF-β1 and activates the TGF-β1 signaling pathway (63,64). The downstream regulation of TGF-β1 is divided into Smad-dependent and Smad-independent signaling pathways (65,66). Following induction by TGF-β1, the downstream transduction molecule Smad2/3 is phosphorylated and activated to form a trimer with Smad4 and conduct the signal from the cell membrane to the nucleus (65). It can activate the production of ECM in the nucleus (67). Previous studies indicated that Smad3-deficient mice show significant inhibition of BLM-induced pulmonary fibrosis (68,69). In contrast, other studies found that the blocking of Smad3 did not entirely weaken the TGF-β1 effect and still played a significant regulatory role in fibrosis (70,71). These findings indicate the existence of other downstream receptors of TGF-β1 to regulate the process of fibrosis. This downstream signaling pathway is called the Smad-independent signaling pathway (72). The ERK/MAPK pathway is a Smad-independent signaling pathway. Previous studies have demonstrated that ERK1/2 can be activated by TGF-β1 in epithelial cells and fibroblasts (73,74) and can stimulate EMT process and ECM production (75,76). In addition, the activation of ERK is necessary for TGF-β1-induced fibroblast replication (77). Notably, a complex cross-talk exists between TGF-β/Smad and TGF-β/ERK pathways. ERK1/2 can phosphorylate the linker region of nuclear-localized Smad, increase the half-life of p-Smad 2/3 and increase the duration of Smad target gene transcription (78,79). In the present study, BLM upregulated the expression of TGF-β1 and increased the phosphorylation levels of Smad2/3 and ERK1/2, which was consistent with previous findings (80). The results indicated that BLM-induced IPF might correspond to the cross-talk between TGF-β/Smad and TGF-β/ERK pathways. Pirfenidone could effectively slow down the progression of IPF in clinical treatment and the mechanism might be related to the regulation of TGF-β/Smad and TGF-β/ERK pathways (81,82). Notably, following the administration of polydatin for 28 days, the rats exhibited a low TGF-β1 level and a significant reduction in Smad2/3 and ERK1/2 phosphorylation, indicating that polydatin could suppress TGF-β/Smad and TGF-β/ERK pathways effectively. In addition, the polydatin high-dose group demonstrated a better inhibition of TGF-β1 expression and phosphorylation of Smad2/3 and ERK1/2 compared with pirfenidone. These pharmacological activities rendered polydatin a broader clinical application value and might account for the protective effect of polydatin against IPF.

The present study demonstrated that polydatin protected against BLM-induced pulmonary fibrosis. The efficacy of polydatin was close to that of resveratrol. The antifibrotic effect of polydatin might be due to the relief from oxidative and inflammatory stress and inhibition of EMT and collagen deposition regulated by Smad-dependent and Smad-independent TGF-β signals. These findings provided new insights into the bioactivity of polydatin. They indicated that polydatin might have therapeutic potential for treating IPF and could also be a promising dietary supplement combined with other clinical antifibrotic drugs.

Acknowledgements

Not applicable.

Funding

The present study was supported by the Pear River Nova Program of Guangzhou (grant no. 201710010075), the Elite Youth Education Program of Guangzhou University of Chinese Medicine and the National Key Research and Development Plan Project 'Special Research Project on Modernization of Traditional Chinese Medicine' (grant no. 2017YFC1703701).

Availability of data and materials

The datasets used and/or analyzed during the current study are available from the corresponding author on reasonable request.

Authors' contributions

ZC, LW and YCL conceived and designed the experiments. YLL, BC, JN and GZ performed the experiments. YLL, BC, JZ and JY analyzed or interpreted the data for the study. YLL and BC drafted the work. ZC, LW and YCL revised the work critically. YLL and BC contributed equally to this work. ZC and LW contributed equally to this work as corresponding authors. All authors read and approved the final manuscript.

Ethics approval and consent to participate

The study was approved by the Animal Protection and Use Committee of Guangzhou University of Chinese Medicine (Guangzhou, China).

Patient consent for publication

Not applicable.

Competing interests

The authors declare that they have no competing interests.

References

1. Luppi F, Spagnolo P, Cerri S and Richeldi L: The big clinical trials in idiopathic pulmonary fibrosis. Curr Opin Pulm Med 18: 428-432, 2012.
2. Wang X, Ouyang Z, You Q, He S, Meng Q, Hu C, Wu X, Shen Y, Sun Y, Wu X and Xu Q: Obaculactone protects against bleomycin-induced pulmonary fibrosis in mice. Toxicol Appl Pharmacol 303: 21-29, 2016.
3. Gouda MM and Bhandary YP: Curcumin down-regulates IL-17A mediated p53-fibrinolytic system in bleomycin induced acute lung injury in vivo. J Cell Biochem 119: 7285-7299, 2018.
4. You XY, Xue Q, Fang Y, Liu Q, Zhang CF, Zhao C, Zhang M and Xu XH: Preventive effects of ecliptae herba extract and its component, ecliptasaponin a, on bleomycin-induced pulmonary fibrosis in mice. J Ethnopharmacol 175: 172-180, 2015.

5. Pardo A and Selman M: Idiopathic pulmonary fibrosis: New insights in its pathogenesis. Int J Biochem Cell Biol 34: 1534-1538, 2002.
6. Manali ED, Stathopoulos GT, Kollintza A, Kalomenidis I, Emili JM, Sotiropoulou C, Daniil Z, Roussos C and Papiris SA: The medical research council chronic dyspnea score predicts the survival of patients with idiopathic pulmonary fibrosis. Respir Med 102: 586-592, 2008.
7. Krein PM and Winston BW: Roles for insulin-like growth factor I and transforming growth factor-beta in fibrotic lung disease. Chest 122 (6 Suppl): 289S-293S, 2002.
8. Handa T and Azuma A: Pharmacotherapy of IPF using antifibrotic compounds. In: Idiopathic Pulmonary Fibrosis. Nakamura H and Aoshiba K (eds). Springer, Japan, pp147-159, 2016.
9. Truong VL, Jun M and Jeong WS: Role of resveratrol in regulation of cellular defense systems against oxidative stress. Biofactors 44: 36-49, 2018.
10. Brasnyó P, Molnár GA, Mohás M, Markó L, Laczy B, Cseh J, Mikolás E, Szijártó IA, Mérei A, Halmai R, *et al*: Resveratrol improves insulin sensitivity, reduces oxidative stress and activates the Akt pathway in type 2 diabetic patients. Br J Nutr 106: 383-389, 2011.
11. Vargas JE, Souto AA, Pitrez PMC, Stein RT and Porto BN: Modulatory potential of resveratrol during lung inflammatory disease. Med Hypotheses 96: 61-65, 2016.
12. Haobo L, Guangfeng Z and Xiao Z: OP0216 resveratrol ameliorates pulmonary fibrosis and inhibits human lung fibroblasts activation via modulating SIRT1 and GLI1 signaling. Ann Rheumatic Diseases 74: 152-153, 2015.
13. Chávez E, Reyes-Gordillo K, Segovia J, Shibayama M, Tsutsumi V, Vergara P, Moreno MG and Muriel P: Resveratrol prevents fibrosis, NF-kappaB activation and TGF-beta increases induced by chronic CCl4 treatment in rats. J Appl Toxicol 28: 35-43, 2008.
14. Di Benedetto A, Posa F, De Maria S, Ravagnan G, Ballini A, Porro C, Trotta T, Grano M, Muzio LL and Mori G: Polydatin, natural precursor of resveratrol, promotes osteogenic differentiation of mesenchymal stem cells. Int J Med Sci 15: 944-952, 2018.
15. Zhang LP, Yang CY, Wang YP, Cui F and Zhang Y: Protective effect of polydatin against ischemia/reperfusion injury in rat heart. Sheng Li Xue Bao 60: 161-168, 2008.
16. Koneru M, Sahu BD, Gudem S, Kuncha M, Ravuri HG, Kumar JM, Kilari EK and Sistla R: Polydatin alleviates alcohol-induced acute liver injury in mice: Relevance of matrix metalloproteinases (MMPs) and hepatic antioxidants. Phytomedicine 27: 23-32, 2017.
17. Cremon C, Stanghellini V, Barbaro MR, Cogliandro RF, Bellacosa L, Santos J, Vicario M, Pigrau M, Alonso Cotoner C, Lobo B, *et al*: Randomised clinical trial: The analgesic properties of dietary supplementation with palmitoylethanolamide and polydatin in irritable bowel syndrome. Aliment Pharmacol Ther 45: 909-922, 2017.
18. Martano M, Stiuso P, Facchiano A, De Maria S, Vanacore D, Restucci B, Rubini C, Caraglia M, Ravagnan G and Lo Muzio L: Aryl hydrocarbon receptor, a tumor grade-associated marker of oral cancer, is directly downregulated by polydatin: A pilot study. Oncol Rep 40: 1435-1442, 2018.
19. Jiang Q, Yi M, Guo Q, Wang C, Wang H, Meng S, Liu C, Fu Y, Ji H and Chen T: Protective effects of polydatin on lipopolysaccharide-induced acute lung injury through TLR4-MyD88-NF-κB pathway. Int Immunopharmacol 29: 370-376, 2015.
20. Liu W, Chen P, Deng J, Lv J and Liu J: Resveratrol and polydatin as modulators of Ca^{2+} mobilization in the cardiovascular system. Ann N Y Acad Sci 1403: 82-91, 2017.
21. Zhang YS, Zhuang ZX, Jiao Y, Xu JY, Fan SJ and Qin SB: Polydatin inhibits metastasis of human breast cancer and underlying mechanisms. China J Cancer Prev Treat 21: 1788-1793, 2014.
22. Pan JH, Wang HB, Du XF, Liu JY and Zhang DJ: Polydatin induces human cervical cancer cell apoptosis via PI3K/AKT/mTOR signaling pathway. Zhongguo Zhong Yao Za Zhi 42: 2345-2349, 2017 (In Chinese).
23. Mo JF, Wu JY, Zheng L, Yu YW, Zhang TX, Guo L and Bao Y: Therapeutic efficacy of polydatin for nonalcoholic fatty liver disease via regulating inflammatory response in obese mice. RSC Adv 8: 31194-31200, 2018.
24. Li R, Li J, Huang Y, Li H, Yan S, Lin J, Chen Y, Wu L, Liu B, Wang G and Lan T: Polydatin attenuates diet-induced nonalcoholic steatohepatitis and fibrosis in mice. Int J Biol Sci 14: 1411-1425, 2018.
25. Shiyu S, Zhiyu L, Mao Y, Lin B, Lijia W, Tianbao Z, Jie C and Tingyu L: Polydatin up-regulates clara cell secretory protein to suppress phospholipase A2 of lung induced by LPS in vivo and in vitro. BMC Cell Biol 12: 31, 2011.
26. Yan XD, Wang QM, Tie C, Jin HT, Han YX, Zhang JL, Yu XM, Hou Q, Zhang PP, Wang AP, *et al*: Polydatin protects the respiratory system from $PM_{2.5}$ exposure. Sci Rep 7: 40030, 2017.
27. Cao K, Lei X, Liu H, Zhao H, Guo J, Chen Y, Xu Y, Cheng Y, Liu C, Cui J, *et al*: Polydatin alleviated radiation-induced lung injury through activation of Sirt3 and inhibition of epithelial-mesenchymal transition. J Cell Mol Med 21: 3264-3276, 2017.
28. Qiu Y, Pan X and Hu Y: Polydatin ameliorates pulmonary fibrosis by suppressing inflammation and the epithelial mesenchymal transition via inhibiting the TGF-β/Smad signaling pathway. RSC Adv 9: 8104-8112, 2019.
29. Gong LK, Li XH, Wang H, Zhang L, Cai Y, Qi XM, Liu LL, Liu YZ, Wu XF, Chen FP, *et al*: Feitai attenuates bleomycin-induced pulmonary fibrosis in rats. Biol Pharm Bull 27: 634-640, 2004.
30. Zhou C, Han W, Zhang P, Cai M, Wei D and Zhang C: Lycopene from tomatoes partially alleviates the bleomycin-induced experimental pulmonary fibrosis in rats. Nutr Res 28: 122-130, 2008.
31. Szapiel SV, Elson NA, Fulmer JD, Hunninghake GW and Crystal RG: Bleomycin-induced interstitial pulmonary disease in the nude, athymic mouse. Am Rev Respir Dis 120: 893-899, 1979.
32. Hübner RH, Gitter W, El Mokhtari NE, Mathiak M, Both M, Bolte H, Freitag-Wolf S and Bewig B: Standardized quantification of pulmonary fibrosis in histological samples. Biotechniques 44: 507-511, 514-517, 2008.
33. Robbe A, Tassin A, Carpentier J, Declèves AE, Mekinda Ngono ZL, Nonclercq D and Legrand A: Intratracheal bleomycin aerosolization: The best route of administration for a scalable and homogeneous pulmonary fibrosis rat model? BioMed Res Int 2015: 198418, 2015.
34. Livak KJ and Schmittgen TD: Analysis of relative gene expression data using real-time quantitative PCR and the 2(-Delta Delta C(T)) method. Methods 25: 402-408, 2001.
35. Zhang F, Zhang Z, Chen L, Kong D, Zhang X, Lu C, Lu Y and Zheng S: Curcumin attenuates angiogenesis in liver fibrosis and inhibits angiogenic properties of hepatic stellate cells. J Cell Mol Med 18: 1392-1406, 2014.
36. Selman M, King TE Jr and Pardo A; American Thoracic Society; European Respiratory Society; American College of Chest Physicians: Idiopathic pulmonary fibrosis: Prevailing and evolving hypotheses about its pathogenesis and implications for therapy. Ann Intern Med 134: 136-151, 2001.
37. Fioret D: Idiopathic pulmonary fibrosis: Diagnosis, management, and the search for a cure. Electronic Theses and Dissertations, University of Louisville. Paper 437: 394, 2012. doi:10.18297/etd/437.
38. McCormack FX, King TE Jr, Voelker DR, Robinson PC and Mason RJ: Idiopathic pulmonary fibrosis. Abnormalities in the bronchoalveolar lavage content of surfactant protein A. Am Rev Respir Dis 144: 160-166, 1991.
39. Williamson JD, Sadofsky LR and Hart SP: The pathogenesis of bleomycin-induced lung injury in animals and its applicability to human idiopathic pulmonary fibrosis. Exp Lung Res 41: 57-73, 2015.
40. Ramirez AM, Wongtrakool C, Welch T, Steinmeyer A, Zügel U and Roman J: Vitamin D inhibition of pro-fibrotic effects of transforming growth factor beta1 in lung fibroblasts and epithelial cells. J Steroid Biochem Mol Biol 118: 142-150, 2010.
41. Yu WN, Sun LF and Yang H: Inhibitory effects of astragaloside IV on bleomycin-induced pulmonary fibrosis in rats via attenuation of oxidative stress and inflammation. Inflammation 39: 1835-1841, 2016.
42. Adegunsoye A, Balachandran J and Ivanovska N: Inflammatory response mechanisms exacerbating hypoxemia in coexistent pulmonary fibrosis and sleep apnea. Mediators Inflamm 2015: 510105, 2015.
43. Hong JS, Ko HH, Han ES and Lee CS: Inhibition of bleomycin-induced cell death in rat alveolar macrophages and human lung epithelial cells by ambroxol. Biochem Pharmacol 66: 1297-1306, 2003.
44. Uchida M, Shiraishi H, Ohta S, Arima K, Taniguchi K, Suzuki S, Okamoto M, Ahlfeld SK, Ohshima K, Kato S, *et al*: Periostin, a matricellular protein, plays a role in the induction of chemokines in pulmonary fibrosis. Am J Respir Cell Mol Biol 46: 677-686, 2012.
45. Li L, Wu W, Huang W, Hu G, Yuan W and Li W: NF-κB RNAi decreases the Bax/Bcl-2 ratio and inhibits TNF-α-induced apoptosis in human alveolar epithelial cells. Inflamm Res 62: 387-397, 2013.

46. Dong SH, Liu YW, Wei F, Tan HZ and Han ZD: Asiatic acid ameliorates pulmonary fibrosis induced by bleomycin (BLM) via suppressing pro-fibrotic and inflammatory signaling pathways. Biomed Pharmacother 89: 1297-1309, 2017.
47. Grounds MD: Complexity of extracellular matrix and skeletal muscle regeneration. Adv Muscle Res 3: 269-302, 2008.
48. Matute-Bello G, Winn RK, Jonas M, Chi EY, Martin TR and Liles WC: Fas (CD95) induces alveolar epithelial cell apoptosis in vivo: Implications for acute pulmonary inflammation. Am J Pathol 158: 153-161, 2001.
49. Hirano Y, Aziz M, Yang WL, Wang Z, Zhou M, Ochani M, Khader A and Wang P: Neutralization of osteopontin attenuates neutrophil migration in sepsis-induced acute lung injury. Crit Care 19: 53, 2015.
50. Van Der Vliet A, Nguyen MN, Shigenaga MK, Eiserich JP, Marelich GP and Cross CE: Myeloperoxidase and protein oxidation in cystic fibrosis. Am J Physiol Lung Cell Mol Physiol 279: L537-L546, 2000.
51. Siqueira RF, Weigel RA, Nunes GR, Mori CS and Fernandes WR: Oxidative profiles of endurance horses racing different distances. Arq Bras Med Vet Zootec 66: 455-461, 2014.
52. Kosters M, Kothari S, Ghaly T and Dhamoon A: Unmasking a rare rheumatological disease with the atypical presentation of acute onset shortness of breath. Chest J 146 (Suppl 4): 414A, 2014.
53. Teixeira KC, Soares FS, Rocha LGC, Silveira PCL, Silva LA, Valença SS, Dal Pizzol F, Streck EL and Pinho RA: Attenuation of bleomycin-induced lung injury and oxidative stress by N-acetylcysteine plus deferoxamine. Pulm Pharmacol Ther 21: 309-316, 2008.
54. Lee YM, Rhee JS, Hwang DS, Kim IC, Raisuddin S and Lee JS: Mining of biomarker genes from expressed sequence tags and differential display reverse transcriptase-polymerase chain reaction in the self-fertilizing fish, kryptolebias marmoratus and their expression patterns in response to exposure to an endocrine-disrupting alkylphenol, bisphenol A. Mol Cells 23: 287-303, 2007.
55. Culcasi M, Benameur L, Mercier A, Lucchesi C, Rahmouni H, Asteian A, Casano G, Botta A, Kovacic H and Pietri S: EPR spin trapping evaluation of ROS production in human fibroblasts exposed to cerium oxide nanoparticles: Evidence for NADPH oxidase and mitochondrial stimulation. Chem Biol Interact 199: 161-176, 2012.
56. Long LL, Yi YJ, Zhou JW, Cheng YD and Xia YB: Microbial transformation of polydatin by endophytic fungi isolated from *polygonum cuspidatum* and antioxidant activity of the products. Mod Food Sci Technol 31: 76-83 and 162, 2015.
57. Massagué J, Blain SW and Lo RS: TGFbeta signaling in growth control, cancer, and heritable disorders. Cell 103: 295-309, 2000.
58. Derynck R and Akhurst RJ: Differentiation plasticity regulated by TGF-beta family proteins in development and disease. Nat Cell Biol 9: 1000-1004, 2007.
59. Branton MH and Kopp JB: TGF-beta and fibrosis. Microbes Infect 1: 1349-1365, 1999.
60. Jin M, Wang L, Wu Y, Zang BX and Tan L: Protective effect of hydroxysafflor yellow A on bleomycin-induced pulmonary inflammation and fibrosis in rats. Chin J Integr Med 24: 32-39, 2018.
61. Khalil N and Greenberg AH: The role of TGF-beta in pulmonary fibrosis. Ciba Found Symp 157: 194-207, discussion 207-211, 1991.
62. Zhou Y, Zhang Q, Gao Y, Tan M, Zheng R, Zhao L and Zhang X: Induced pluripotent stem cell-conditioned medium suppresses pulmonary fibroblast-to-myofibroblast differentiation via the inhibition of TGF-β1/Smad pathway. Int J Mol Med 41: 473-484, 2018.
63. Tobar N, Villar V and Santibanez JF: ROS-NFkappaB mediates TGF-beta1-induced expression of urokinase-type plasminogen activator, matrix metalloproteinase-9 and cell invasion. Mol Cell Biochem 340: 195-202, 2010.
64. Verrecchia F and Mauviel A: TGF-beta and TNF-alpha: Antagonistic cytokines controlling type I collagen gene expression. Cell Signal 16: 873-880, 2004.
65. Feng XH and Derynck R: Specificity and versatility in TGF-beta signaling through Smads. Annu Rev Cell Dev Biol 21: 659-693, 2005.
66. Derynck R and Zhang YE: Smad-dependent and Smad-independent pathways in TGF-beta family signalling. Nature 425: 577-584, 2003.
67. Roberts AB, Tian F, Byfield SD, Stuelten C, Ooshima A, Saika S and Flanders KC: Smad3 is key to TGF-beta-mediated epithelial-to-mesenchymal transition, fibrosis, tumor suppression and metastasis. Cytokine Growth Factor Rev 17: 19-27, 2006.
68. Zhao J, Shi W, Wang YL, Chen H, Bringas P Jr, Datto MB, Frederick JP, Wang XF and Warburton D: Smad3 deficiency attenuates bleomycin-induced pulmonary fibrosis in mice. Am J Physiol Lung Cell Mol Physiol 282: L585-L593, 2002.
69. Shou J, Cao J, Zhang S, Sun R, Zhao M, Chen K, Su SB, Yang J and Yang T: SIS3, a specific inhibitor of smad3, attenuates bleomycin-induced pulmonary fibrosis in mice. Biochem Biophys Res Commun 503: 757-762, 2018.
70. Wang S, Wilkes MC, Leof EB and Hirschberg R: Imatinib mesylate blocks a non-Smad TGF-beta pathway and reduces renal fibrogenesis in vivo. FASEB J 19: 1-11, 2005.
71. Zhang M, Fraser D and Phillips A: ERK, p38, and Smad signaling pathways differentially regulate transforming growth factor-beta1 autoinduction in proximal tubular epithelial cells. Am J Pathol 169: 1282-1293, 2006.
72. Chun JN, Park S, Lee S, Kim JK, Park EJ, Kang M, Kim HK, Park JK, So I and Jeon JH: Schisandrol B and schisandrin B inhibit TGFβ1-mediated NF-κB activation via a Smad-independent mechanism. Oncotarget 9: 3121-3130, 2017.
73. Hartsough MT and Mulder KM: Transforming growth factor beta activation of p44mapk in proliferating cultures of epithelial cells. J Biol Chem 270: 7117-7124, 1995.
74. Mucsi I, Skorecki KL and Goldberg HJ: Extracellular signal-regulated kinase and the small GTP-binding protein, Rac, contribute to the effects of transforming growth factor-beta1 on gene expression. J Biol Chem 271: 16567-16572, 1996.
75. González MN, de Mello W, Butler-Browne GS, Silva-Barbosa SD, Mouly V, Savino W and Riederer I: HGF potentiates extracellular matrix-driven migration of human myoblasts: Involvement of matrix metalloproteinases and MAPK/ERK pathway. Skelet Muscle 7: 20, 2017.
76. Hu X, Wang H, Liu J, Fang X, Tao K, Wang Y, Li N, Shi J, Wang Y, Ji P, *et al*: The role of ERK and JNK signaling in connective tissue growth factor induced extracellular matrix protein production and scar formation. Arch Dermatol Res 305: 433-445, 2013.
77. Hough C, Radu M and Doré JJ: TGF-beta induced Erk phosphorylation of smad linker region regulates smad signaling. PLoS One 7: e42513, 2012.
78. Matsuura I, Wang G, He D and Liu F: Identification and characterization of ERK MAP kinase phosphorylation sites in Smad3. Biochemistry 44: 12546-12553, 2005.
79. Kretzschmar M, Doody J, Timokhina I and Massagué J: A mechanism of repression of TGFbeta/Smad signaling by oncogenic Ras. Genes Dev 13: 804-816, 1999.
80. Wang G, Jiao H, Zheng JN and Sun X: HSP27 regulates TGF-β mediated lung fibroblast differentiation through the Smad3 and ERK pathways. Int J Mol Med 39: 183-190, 2017.
81. Conte E, Gili E, Fagone E, Fruciano M, Iemmolo M and Vancheri C: Effect of pirfenidone on proliferation, TGF-β-induced myofibroblast differentiation and fibrogenic activity of primary human lung fibroblasts. Eur J Pharm Sci 58: 13-19, 2014.
82. Li C, Rezov V, Joensuu E, Vartiainen V, Rönty M, Yin M, Myllärniemi M and Koli K: Pirfenidone decreases mesothelioma cell proliferation and migration via inhibition of ERK and AKT and regulates mesothelioma tumor microenvironment in vivo. Sci Rep 8: 10070, 2018.